# Determination of the Intra- and Intermolecular Microstructure of Bulk and Emulsion Copolymers of Styrene and 2-Hydroxyethyl Methacrylate by Means of Proton NMR and Gradient Polymer Elution Chromatography

**Harold A. S. Schoonbrood,† Annemieke M. Aerdts, and Anton L. German***

*Laboratory of Polymer Chemistry and Technology, Eindhoven University of Technology, P.O. Box 513, 5600 MB Eindhoven, The Netherlands*

**Geert P. M. van der Velden**

*DSM Research B.V., P.O. Box 18, 6160 MD Geleen, The Netherlands*

*Received December 1, 1994; Revised Manuscript Received April 17, 1995*®

ABSTRACT: A series of copolymers of styrene and 2-hydroxyethyl methacrylate was prepared with free-radical bulk copolymerization at 50 °C and analyzed with proton NMR to determine the reactivity ratios according to the terminal model and to study the intramolecular microstructure. The reactivity ratios were analyzed with a noniterative nonlinear least-squares method ($r_H = 0.48 \pm 0.15$ and $r_S = 0.27 \pm 0.08$) and the so-called error-in-variables method ($r_H = 0.49$ and $r_S = 0.27$). The hydroxyl proton resonance signal was found to be sensitive to the copolymer composition and could be interpreted in terms of compositional and configurational sequence effects. An assignment was proposed which is comparable to the assignments made for the methoxy protons of styrene–methyl acrylate copolymers. The coisotacticity parameter $\sigma_{HS}$ was calculated using a nonlinear least-squares procedure with relative error estimation based on the current assignment and was found to be 0.33. With gradient polymer elution chromatography (chemical composition distribution) and with proton NMR, the inter- and intramolecular microstructures, respectively, of three emulsion copolymers of styrene and 2-hydroxyethyl methacrylate were studied. By using the chemical composition distribution and comparing the hydroxyl proton signal of these emulsion copolymers to that of a bulk copolymer with the same overall composition, it could be shown convincingly that styrene and 2-hydroxyethyl methacrylate copolymerize during the greater part of the emulsion polymerization.

## Introduction

High-resolution nuclear magnetic resonance (NMR) spectroscopy has been particularly effective in the determination of the microstructure of copolymers, both intermolecular (average or cumulative chemical composition) and, especially, intramolecular (sequence distribution and tacticity). Sometimes even the intermolecular microstructure in terms of the chemical composition distribution (CCD) can be determined with NMR, if the cumulative composition is measured as a function of conversion. Schoonbrood *et al.*[1,2] did this for an emulsion terpolymer of styrene, methyl methacrylate, and methyl acrylate. The knowledge of the copolymer microstructure is important from two perspectives: (1) the information that it provides on the reaction mechanism occurring during polymerization and (2) the key role that it plays in the understanding of relations between the polymerization mechanism, molecular structure, and properties.[3,4]

In many NMR studies of copolymers attention has been paid to the microstructural analysis of the proton NMR spectra of styrene–methyl methacrylate copolymers (S–MMA)[5] and also of the carbon NMR spectra of the same system.[6] Other styrene–(meth)acrylate systems which have been successfully described in terms of intramolecular microstructure are styrene–ethyl methacrylate (S–EMA),[7] styrene–methyl acrylate (S–MA),[8] styrene–ethyl acrylate (S–EA),[9] and styrene–butyl acrylate (S–BA).[10] In all cases the methoxy proton resonance signal was interpreted in terms of compositional and configurational sequence effects. The methoxy resonance signals in the proton spectra of the styrene–methacrylate copolymers are complex, and overlapping occurs between the methoxy protons and other main-chain resonances, which is not the case with the methoxy resonance signals in the proton spectra of the styrene–acrylate copolymers.[9]

The present work focuses on the system styrene–2-hydroxyethyl methacrylate (S–HEMA) copolymerizing at 50 °C. In a preliminary report,[11] one of the present authors studied the proton NMR and the carbon MAS solid-state NMR spectra of this system. However, the report was focused on the curing behavior of networks of S–HEMA and Desbimid, which is a mixture of bis(maleimide), maleimide–isomaleide, maleimide–acetamide, and maleic anhydride. Proton NMR spectra of S–HEMA copolymers were measured in a rather limited region of molar ratios; the copolymers had a limited solubility due to the fact that the monomers were not purified. Besides this report there are no publications dealing with the S–HEMA copolymer characterization in terms of compositional and configurational sequence distribution. Investigations of other copolymers with HEMA as one of the comonomers are also rare. Gallardo and San Román[12] studied the microstructure of copolymers of HEMA and *N*-[4-(methacryloyloxy)-phenyl]-2-(4-methoxyphenyl)acetamide with proton and carbon NMR. In the same group the copolymer of 4-(methacryloyloxy)acetanilide (MOA) and HEMA[13,14] was also studied in terms of intramolecular microstructure, whereas the glycidyl methacrylate–HEMA copoly-

* To whom correspondence should be addressed.
† Present address: Grupo de Ingeniería Química, Departamento de Química, Aplicada, Facultad de Ciencias Químicas, Universidad del País Vasco, Apartado 1072, 20080 San Sebastián, Spain.
® Abstract published in *Advance ACS Abstracts,* June 15, 1995.

0024-9297/95/2228-5518$09.00/0 

mer system was only studied to determine the reactivity ratios.[15]

Although attention for the microstructure of S–HEMA copolymers has been very limited, the determination of reactivity ratios of the comonomer pair S–HEMA in various solvents has been reported often in literature, *e.g.*, ref 16. Galbraith *et al.*[17] collected the reactivity ratios determined by various authors, but none of these reactivity ratios pertain to the bulk polymerization at 50 °C. In most cases HEMA is found to be the more reactive monomer, with the reactivity ratios of both monomers mostly being smaller than unity, which means that random copolymers are formed. Additionally, Lebduška *et al.*[18] studied the total copolymerization rate of the solution copolymerization of S and HEMA in various solvents at 60 °C by dilatometry.

From the perspective of emulsion polymerization the comonomer system S–HEMA is interesting, because S is a sparsely water-soluble monomer and HEMA is completely miscible in water.[1,19] This combination often leads to strong composition drift and in extreme cases to considerable homopolymerization of one or both of the monomers such as was reported copolymerization of S with acrylamide.[20] In literature, limited attention has been paid to the emulsion polymerization of S and HEMA.[19] Kamei *et al.*[21] performed emulsifier-free emulsion copolymerizations (at 70 °C) of S with various amounts of HEMA, up to 20 mol %, and noted that the polymer particles exhibited anomalous, nonspherical shapes. Up to 30% conversion they observed an increased consumption rate of HEMA, which was attributed to aqueous phase polymerization, and above 30% conversion they observed an increased S consumption rate. This, they argued, leads to the formation of a HEMA-rich copolymer and a S-rich copolymer, which do not mix. However, no further experimental evidence for this mechanism was given. Okubo *et al.*[22] also studied the emulsifier-free emulsion copolymerization of S and HEMA, and they used X-ray photoelectron spectroscopy to determine the particle surface concentration of HEMA. The surface was found to be enriched in HEMA, which they explained by invoking a two-step emulsion polymerization rather than an emulsion copolymerization, which would lead to phase separation, with the HEMA-rich copolymer at the surface. However, again no further experimental evidence for this mechanism was given. So, at this point virtually nothing is known about the emulsion copolymerization mechanism with appreciable amounts of HEMA. This emulsion copolymerization can be important for the preparation of reactive latices with primary hydroxyl groups. These latices are of special interest because of their use in post-cross-linkable latex systems, where they are mixed with another latex bearing complementary reactivity. In this respect it is not favorable that HEMA does not copolymerize with its comonomer. In this paper we, therefore, attempt to clarify whether copolymerization with S does take place.

The proton NMR spectra of low-conversion S–HEMA bulk copolymers will be used for the determination of the reactivity ratios of this comonomer pair at 50 °C. The same copolymers will be used to study the intramolecular microstructure by looking in detail at the hydroxyl proton signals. In the previously mentioned systems S–MA, S–MMA, and S–EMA, the methylene protons of the ester group were studied. In this case, however, the two pairs of methylene protons in the ester group were not exclusively studied, because both methylene groups (R = $CH_2OH$) strongly overlap mutually and also with the water resonance. We, therefore, preferred to study the hydroxyl resonances of the S–HEMA copolymer in detail, because these exhibit a 3-fold splitting in the polar solvent dimethyl sulfoxide. Such phenomena have also been observed for ethylene–vinyl alcohol[23] and vinyl acetate–vinyl alcohol copolymers.[24] For polar copolymers like S–(meth)acrylic acid and S–(meth)acrylamide copolymers, no such splitting has been observed in the literature.[25–28] San Román *et al.*[14] studied the system MOA–HEMA with proton NMR and carbon NMR but observed no splitting of the hydroxyl signal in proton NMR.

The assignments used here for the hydroxyl proton of S–HEMA are comparable with those of the methoxy proton of styrene–acrylate copolymers.[8] This will enable the determination of the sequence distributions and stereoregularity. The results of the study of the intramolecular microstructure of the bulk copolymers of S and HEMA will be applied to the emulsion copolymerization of these monomers at 50 °C.

As stated before, the polymerization mechanism has not been elucidated clearly yet, and an attempt will be made here to do so by determining the intermolecular microstructure (chemical composition distribution) with gradient polymer elution chromatography (GPEC; see the Experimental Section) and in a more elegant way by determining the intramolecular microstructure (sequence distribution, more specifically, the hydroxyl proton resonances in the NMR spectra of these emulsion copolymers) and comparing this with the intramolecular microstructure of the corresponding bulk copolymers. This is an exhaustive study of the emulsion copolymerization of S and HEMA, but it rather serves as an example of the possibility to use NMR and the intramolecular microstructure to deduce conclusions about polymerization mechanisms.

## Experimental Section

The monomers styrene (S) and 2-hydroxyethyl methacrylate (HEMA) (both Merck, p.a.) were distilled at reduced pressure and stored at 4 °C.

**Bulk Copolymerization.** The bulk copolymers were synthesized in 200-mL thermostated glass vessels. The temperature was 50 °C. A free-radical initiator, α,α′-azobis(isobutyronitrile) (AIBN), was used (0.5 wt % of the monomers). The monomers were weighed into the reactor vessels and purged with nitrogen. The conversion was monitored by withdrawing samples with a syringe and adding them to excess nonsolvent (water and acetone at ratios depending on the monomer/copolymer composition). As soon as some precipitate was observed, the reaction mixtures were short-stopped with hydroquinone. Conversion was always lower than 6%. The polymer was separated from the monomers by subsequent cycles of pouring into excess nonsolvent, decanting, and redissolving in a solvent. The copolymers were dried under reduced pressure at 50 °C.

**Emulsion Copolymerizations.** Three batch emulsion copolymerizations of S and HEMA were carried out in a stainless steel reactor of 1.3 $dm^3$. All reactions were carried out at 50 °C with the following recipes (per 100 g of water): sodium dodecyl sulfate (emulsifier, Fluka, 99%), *ca.* 0.11 g; sodium persulfate (initiator), *ca.* 0.03 g; sodium bicarbonate (buffer), *ca.* 0.01 g; *n*-dodecyl mercaptan (chain-transfer agent), 1 wt % of monomer (all Merck, p.a.). The monomer to water ratios (M/W) were varied.

**NMR Experiments.** The proton NMR spectra were recorded with a 400-MHz (Bruker AM 400) spectrometer at 25 °C with DMSO-$d_6$ as the solvent and locking agent. The spectra were obtained using a spectral width of 6024 Hz, an acquisition time of 2.7 s, a flip angle of 60°, and a pulse decay

of 4.8 s. Spectra were obtained after accumulating 32 scans, by using a sample concentration of 1% (w/v). The digital resolution amounted to 0.18 Hz, corresponding to a data length of 32K. Monomer sequence placements were determined by comparing the relative peak areas of the proton atoms involved. When performing quantitative NMR measurements via compositional or configurational sequence placements, it may be necessary to take into account differences in nuclear Overhauser effects (NOE) and spin–lattice relaxation times ($T_1$), but no differential NOEs were considered to occur here. Under these conditions the relative peak areas were determined, after truncation of overlapping spectral regions, numerically (for the overall composition) or with a planimeter (for the hydroxyl region).

**Gradient Polymer Elution Chromatography (GPEC).** (GPEC is a commercial trade name of Waters.) A mixture of copolymers or copolymer chains with varying chemical composition can be separated and analyzed with gradient polymer elution chromatography (GPEC), which allows the determination of the chemical composition distribution (CCD). It is a distinct form of liquid chromatography that is used to separate copolymers with varying chemical composition by eluting with a solvent–nonsolvent eluent mixture with a time-dependent gradient in solvent strength. A sample of a copolymer is dissolved in a good solvent (a good solvent for all polymer chains in the sample). This is injected in the eluent with a high content of nonsolvent. This results in separation in a dilute phase, which is taken up by the eluent, and in a polymer-rich phase, which adheres to the column. The composition of the eluent is gradually changed and the content of the good solvent increased (hence gradient elution). As the eluent contains more solvent, the separation process is reversed and more and more chains are taken up by the eluent and eluted through the column, until finally all chains have been redissolved and eluted. The chains are separated at varying elution times corresponding to the solvent composition at which they are soluble. The polymer chains are separated on the basis of changing solvent/nonsolvent ratios needed to dissolve a chain. These ratios are determined mainly by the microstructure of a chain, in most cases completely determined by the composition. As usual, ideal conditions are very rare, and there will almost always be some influence of the degree of polymerization. This effect is minimal at high degrees of polymerization, say >100. If composition drift occurs during a free-radical polymerization, the changes in monomer composition are negligible on the time scale of chain growth, so the intramolecular structure of a chain is homogeneous, *i.e.*, not dependent on the degree of polymerization. The procedure for the separation of the copolymers has been described elsewhere.[29] A C18 column (Nova-Pak C18, Waters, 3.9 mm × 15 cm) and an evaporative light-scattering detector (ELSD; Model 750/14, Applied Chromatography Systems Ltd.) were used. In this detector the eluent is nebulized by a nitrogen flow. This flow is then heated and the eluent evaporated. An aerosol is formed of the nonvolatiles (polymer), and this is detected with light scattering. Though the detector response may depend slightly on the chemical composition of the chains, it is practically proportional to the mass. The elution gradient was started with a water/methanol mixture (80/20, v/v) at constant composition for 1 min. The eluent composition was then linearly changed to tetrahydrofuran/methanol (80/20, v/v) over a period of 80 min and kept at that ratio for 5 min. The flow rate was 0.9 cm$^3$/min. The calibration (linking retention time to chemical composition) was performed with a mixture of the low-conversion bulk copolymers used in the NMR study, a high molecular weight sample of poly(HEMA) (Polyscience Scientific Polymer Products Inc.), and a high molecular weight poly(S). The chemical composition was fitted with a second-order polynomial to the retention time.

**Calculations.** The reactivity ratios were determined with two numerical techniques: (1) a simple noniterative nonlinear least-squares fitting procedure (NINLLS) with absolute error estimation[30] and (2) the error-in-variables model (EVM).[31] Monomer compositions used to determine the reactivity ratios were varied over a wide range, although it is realized that this may not be the best statistical method for *parameter estimation* according to Tidwell and Mortimer,[32] which is by replicating experiments at two well-chosen compositions.

The coisotacticity parameter $\sigma_{HS}$ was calculated using a nonlinear least-squares procedure with relative error estimation.[30]

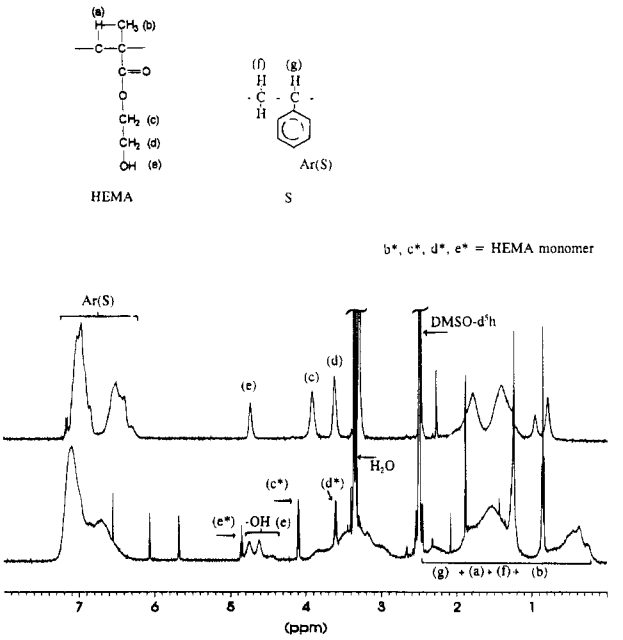


**Figure 1.** 400-MHz proton NMR spectrum (bottom) of a low-conversion bulk S–HEMA copolymer in DMSO at 25 °C with a mole fraction of HEMA ($F_H$) of 0.35 and (top) of a physical mixture of the two homopolymers poly(S) (low molecular weight) and poly(HEMA) in DMSO at 25 °C ($F_H$ = 0.21).

**Table 1. Molar Feed Composition ($f_H$), Experimentally Determined Copolymer Composition (Proton NMR) ($F_H$), and Conversion ($x_0$) of the Low-Conversion Bulk Copolymers**

| $f_H$ | $F_H$ | $x_0$ (%) |
|---|---|---|
| 0.098 | 0.24 | 2.4 |
| 0.200 | 0.35 | 3.4 |
| 0.300 | 0.41 | 2.2 |
| 0.400 | 0.46 | 3.9 |
| 0.600 | 0.62 | 0.2 |
| 0.700 | 0.63 | 1.7 |
| 0.800 | 0.73 | 5.8 |
| 0.901 | 0.85 | 2.9 |

## Results and Discussion

**Low-Conversion S–HEMA Bulk Copolymers.** *Determination of the Copolymer Composition and the Reactivity Ratios.* Figure 1 shows a typical example of a 400-MHz proton NMR spectrum of a low-conversion bulk S–HEMA copolymer dissolved in DMSO-$d_6$ at 25 °C. For comparison the NMR spectrum of a physical mixture of the two pertaining homopolymers is also shown. Note that the poly(S) in the physical mixture is of very low molecular weight, hence the typical structure of the aromatic proton signal. The average copolymer composition (mole fraction HEMA, $F_H$) can be readily obtained by using

$$F_H = \frac{5A_H}{5A_H + A_A} \tag{1}$$

where $A_H$ and $A_A$ represent the total peak areas of the hydroxyl and the aromatic proton resonances, respectively. Eight low-conversion bulk copolymerizations were carried out, and the results are shown in Table 1,

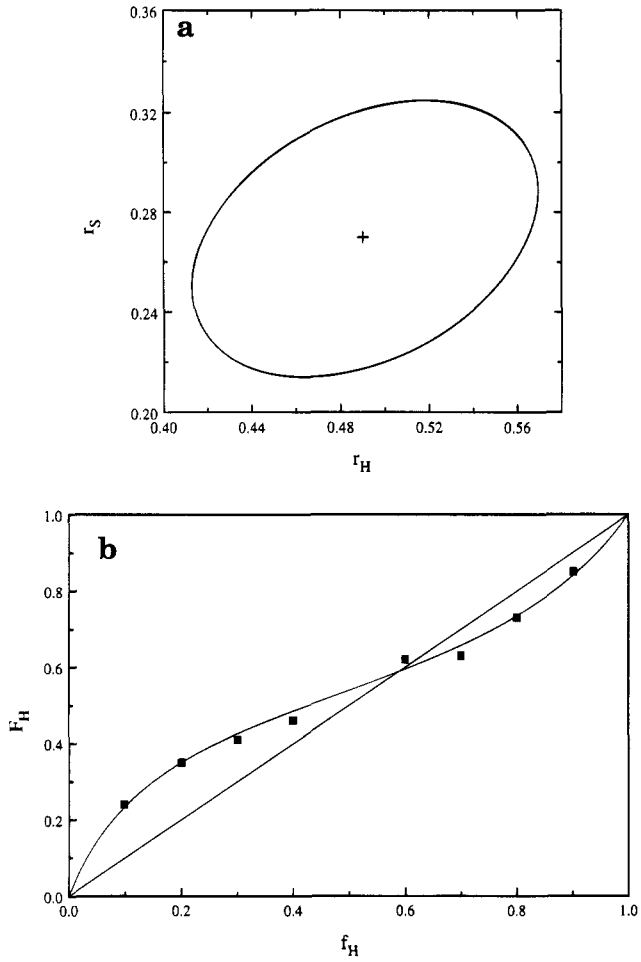


**Figure 2.** (a) 95% joint confidence region of the reactivity ratios of the bulk copolymerization of S and HEMA, as determined with the EVM method. (b) Experimental NMR data (copolymer composition $F_H$ versus monomer composition $f_H$) of the low-conversion bulk copolymers of S and HEMA, and the fit with the terminal model with $r_H = 0.49$ and $r_S = 0.27$.

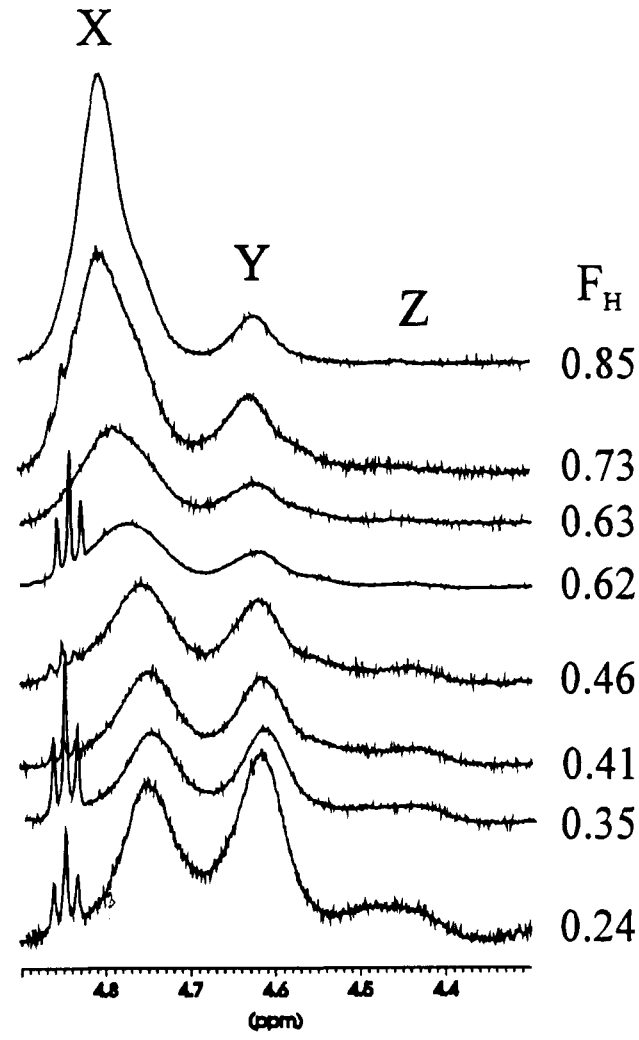


**Figure 3.** Expanded 400-MHz proton NMR spectra of eight low-conversion bulk S–HEMA copolymers showing the hydroxyl region only. Spectra were recorded in DMSO at 25 °C. Area measurements have been performed for the regions X, Y, and Z. The copolymer compositions are indicated on the right.

where the initial molar feed composition ($f_H$), the average copolymer composition ($F_H$), and the conversion ($x_0$) are given.

The reactivity ratios for the AIBN-initiated system at 50 °C were determined according to the two methods mentioned in the Experimental Section. The resulting values are $r_H = 0.48 \pm 0.15$ and $r_S = 0.27 \pm 0.08$ for the NINLLS method and $r_H = 0.49$ and $r_S = 0.27$ for the EVM method with a 95% confidence region as depicted in Figure 2a.

In Figure 2b are depicted the experimental composition data and the line calculated with the reactivity ratios obtained after fitting the data. It can be seen that the data are fitted very well.

*Peak Assignment and Sequence Analysis.* In the analysis of the proton NMR spectra of the low-conversion S–HEMA bulk copolymers, we focused on the hydroxyl resonance of the 2-hydroxylethyl group. The signals of both sets of methylene protons of this group are assumed to be influenced by both sequence and tacticity. However, it appears that severe mutual overlap occurs for these resonances. Moreover, as is evident from Figure 1, overlap occurs with the resonance of the $H_2O$, present in the NMR solvent. We therefore decided to concentrate on the hydroxyl resonance only.

The hydroxyl resonances are split up. This is a consequence of a subtle balance between sample concentration, measurement temperature, and the acidity of the NMR solution (in DMSO-$d_6$). From our practice[33] we know that especially at dilute solutions in DMSO-$d_6$ split up of the hydroxyl resonances is observed. Similar splittings are observed for poly(vinyl alcohol),[34] ethylene–vinyl alcohol copolymers,[23] vinyl acetate–vinyl alcohol copolymers,[24] and ethylene–vinyl alcohol–vinyl chloride terpolymers,[35] all of them recorded in DMSO-$d_6$ dilute solutions. Such phenomena have not been observed for systems like S–(meth)acrylic acid or S–(meth)acrylamide copolymers.[25–28]

In Figure 3 expanded 400-MHz spectra are shown of eight low-conversion S–HEMA bulk copolymers. The expansions of the hydroxyl proton region are shown since, in particular, this region displays additional fine splittings, varying considerably with copolymer composition. These fine splittings of the hydroxyl proton signal were not observed in copolymers of HEMA with *N*-[(4-methacryloyloxy)phenyl]-2-(4-methoxyphenyl), a methacrylic ester,[12] or in copolymers of HEMA with methyl acrylate in DMSO-$d_6$.[36] The hydroxyl proton resonance signal in S–HEMA copolymers appears to consist of three distinctive peaks in the regions of X = 4.9–4.7 ppm, Y = 4.7–4.52 ppm, and Z = 4.52–4.35 ppm. There are three kinds of triads along the copolymer chain, having a 2-hydroxyethyl methacrylate unit in the center: HHH, HHS/SHH, and SHS, where H and

S represent 2-hydroxyethyl methacrylate and styrene units, respectively. By looking carefully at the expanded spectra, the following could be concluded. No configurational effects are observed in the proton NMR spectrum of poly(HEMA) in the presence of homopolymer poly(S) (Figure 1), so all the different configurational HHH triads resonate at peak X. Therefore, we assume that the chemical shift differences only occur in the configuration of neighboring S and H units. There are no solvent or concentration effects, so the resolved hydroxyl resonances can be clarified due to shielding by neighboring coisotactic S units. This means that we can distinguish six different compositional and configurational sequences to be determined in the proton NMR spectra, i.e., HHH, $\sigma_{HS}$ HHS, $(1 - \sigma_{HS})$ HHS, $\sigma_{HS}^2$ SHS, $2\sigma_{HS}(1 - \sigma_{HS})$ SHS, and $(1 - \sigma_{HS})^2$ SHS, where $\sigma_{HS}$ is the coisotacticity parameter, which is defined as the probability that alternating H and S units adopt a coisotactic configuration. Moreover, it is assumed that there are no chemical shift differences between HHS and SHH triads. The hydroxyl proton resonance of a HEMA-centered triad is resolved due to shielding by a neighboring coisotactic S unit. We assumed that shielding by an aromatic ring opposite to the HEMA unit is very small. This means that, due to a long-range diamagnetic shielding effect by phenyl rings, the hydroxyl proton of a central H unit in an isotactic HHS triad may appear at a somewhat higher field than that due to a HHH triad. Almost no differences in chemical shift will be observed for the heterotactic HHS triad and for the heterotactic SHS triad. From Figure 3 (at high mole fractions of styrene in the copolymer) it becomes obvious that the three different configurational SHS triads should be assigned to peaks X, Y, and Z and that the isotactic SHS resonates at peak Z. The following peak assignment is proposed:[37]

$$F_X = F_{HHH} + (1 - \sigma_{HS})F_{HHS} + (1 - \sigma_{HS})^2 F_{SHS} \quad (2a)$$

$$F_Y = \sigma_{HS}F_{HHS} + 2\sigma_{HS}(1 - \sigma_{HS})F_{SHS} \quad (2b)$$

$$F_Z = \sigma_{HS}^2 F_{SHS} \quad (2c)$$

Thus the same compositional and configurational sequence effects as for the $OCH_3$ resonance in the (*S*)-methyl acrylate copolymers[8,37] are observed, leading to the same assignment.

With increasing HEMA content both peak X and more moderately Y are shifted to lower field, due to a combination of the sequence assignments. The sequence HHH is assigned to lowest field, so with increasing HEMA this signal becomes more important. Peak Z cannot be quantitatively considered for compositions higher than $F_H = 0.63$.

This assignment can be verified quantitatively. For this purpose the experimental values of $F_X$, $F_Y$, and $F_Z$ need to be compared with theoretical values. These can be obtained with eq 2a–c, for which the theoretical values of the triad fractions $F_{HHH}$, $F_{HHS}$, and $F_{SHS}$ and the coisotacticity parameter $\sigma_{HS}$ are needed. $\sigma_{HS}$ is not known and will be an adjustable parameter. The theoretical values of the three triad fractions can be calculated easily with an appropriate propagation model, in this case the terminal model (first-order Markov statistics). By assuming this model to be valid, the following equations can be derived for the triad fractions:

$$F_{HHH} = P(H/H)^2 \quad (3a)$$

$$F_{HHS} = P(H/H)(1 - P(H/H)) \quad (3b)$$

$$F_{SHS} = (1 - P(H/H))^2 \quad (3c)$$

where $F$ represents the number fractions of triads normalized to unity and $P(H/H)$ is the probability of a HEMA-terminated growing polymer chain to react with monomer HEMA. $P(H/H)$, the probability of a given HEMA unit being followed by another HEMA unit, is given by:

$$P(H/H) = (r_H/q)/(1 + r_H/q) \quad (4)$$

with $r_H$ as the monomer reactivity ratio of HEMA and $q$ as the molar feed ratio S/HEMA.

With the experimental molar feed ratios $q$ and the reactivity ratios determined earlier, the theoretical values for the triad fractions are calculated with eqs 3a–c and 4 (see Table 2). The coisotacticity parameter can then be calculated with a nonlinear least-squares procedure with relative error estimation[30] by using experimental values for $F_X$, $F_Y$, and $F_Z$ and theoretically calculated values for $F_{HHH}$, $F_{HHS}$, and $F_{SHS}$ and eq 2a–c. A coisotacticity parameter of $0.33 \pm 0.05$ was found.

*Comparison of Theoretical Predictions and Experimental Values of the Triad Fractions.* The experimental peak areas of the hydroxyl proton resonances ($F_X$, $F_Y$, $F_Z$) are compared with theoretical peak areas calculated via eq 2a–c. The results are presented in Table 2 also. The good agreement between the experimental and theoretical values indicates the correctness of the assignment proposed for the hydroxyl proton resonances.

**Microstructure of High-Conversion S–HEMA Emulsion Copolymers.** Now that the hydroxyl proton resonances of the bulk copolymers have been interpreted, it is possible to study other S–HEMA copolymers. As stated in the introduction, S–HEMA copolymers prepared in emulsion are interesting because HEMA is water-miscible and because it bears a functional group, which is important in post-cross-linkable latices. It has been shown that the monomer partitioning behavior of systems with this completely water-miscible monomer is very different from that of systems with only low to moderately water-soluble monomers.[1] From the reactivity ratios it can be concluded that HEMA is more reactive than S in bulk. On the other hand, HEMA is water-miscible, and this will counteract the effect of reactivity on composition drift, and it has been suggested that in this emulsion copolymerization system two homopolymerizations take place: the formation of a HEMA-rich copolymer at the beginning and a S-rich copolymer at the end[21,22] or even the formation of poly(HEMA) in the aqueous phase and poly(S) in the polymer phase concurrently. This is further investigated in the following section.

*Copolymerization Mechanism in the Emulsion Copolymerization of S and HEMA.* In Figure 4 the CCDs of three S–HEMA emulsion copolymers with varying monomer to water ratios (M/W) are shown. It can be seen that the distributions are probably bimodal, with a copolymer very rich in S and some polymeric/oligomeric material that, according to the calibration, is eluted from the column before the high molecular weight poly(HEMA), which was used as a standard for $F_S = 0$. With the gradient used here, HEMA-rich polymers elute first. As HEMA is very water-soluble, water-miscible

**Table 2. Molar Feed Fractions ($f_H$), Monomer Feed Ratios ($q$), and Observed, Normalized Area Intensities of Peaks X, Y, and Z Representing the Hydroxyl Proton Region and the Calculated Values of X, Y, and Z Using Ito's Assignment of Some Low-Conversion Bulk S–HEMA Copolymers**

| | | observed | | | Ito's assignment ($\sigma_{HS}$ = 0.33) | | |
|---|---|---|---|---|---|---|---|
| $f_H$ | $q$ | X | Y | Z | X | Y | Z |
| 0.098 | 0.109 | 0.43 | 0.45 | 0.12 | 0.47 | 0.43 | 0.10 |
| 0.200 | 0.250 | 0.48 | 0.42 | 0.10 | 0.50 | 0.41 | 0.09 |
| 0.300 | 0.429 | 0.51 | 0.41 | 0.08 | 0.53 | 0.40 | 0.07 |
| 0.400 | 0.668 | 0.52 | 0.41 | 0.07 | 0.56 | 0.38 | 0.06 |
| 0.600 | 1.50 | 0.64 | 0.33 | 0.03 | 0.65 | 0.31 | 0.04 |
| 0.700 | 2.33 | 0.68 | 0.29 | 0.03 | 0.71 | 0.26 | 0.03 |
| 0.800 | 4.00 | 0.74 | 0.24 | 0.02 | 0.79 | 0.20 | 0.01 |
| 0.901 | 9.12 | 0.85 | 0.13 | 0.02 | 0.88 | 0.11 | 0.01 |

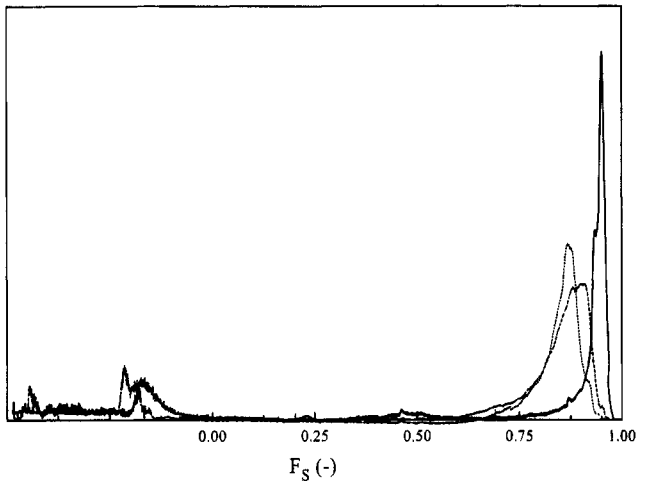


**Figure 4.** Three CCDs of S–HEMA emulsion copolymers with $F_S$ = 0.75 and with varying M/W: 0.05 (—), 0.2 (- - -), and 0.5 (• • •), as determined with GPEC/ELSD. The label for the $y$-axis is relative mass.

in fact, and styrene is just sparingly water-soluble, it is possible that in the aqueous phase a homopolymer of HEMA is formed. As there can be considerable termination in the aqueous phase, this material probably has a low molecular weight. Because low molecular weight polymers can have a different retention behavior than high molecular weight polymers, *i.e.*, they normally elute earlier, this may account for their shorter retention time and hence the apparently negative value of $F_S$. Cross-fractionation with GPEC followed by gel permeation chromatography might prove very useful. The different positions of the S-rich copolymer peaks show that the compositions of these polymers depend on M/W: the higher M/W, the more the peaks are shifted to higher HEMA fractions. This is what one would expect if S and HEMA copolymerize mainly in the particles: the higher M/W, the less HEMA is retained in the aqueous phase and the more it is present in the particles.

Figure 5, where the cumulative fraction of S ($F_{S,c}$) in the copolymer is plotted versus conversion for the three emulsion copolymerizations with varying M/W, reveals that in the first stage of the reactions HEMA is consumed faster than S but that after a conversion of 10–20% the consumption of S has increased noticeably. At the end, the relative consumption rate of HEMA must again be higher than that of S in the cases of M/W = 0.05 and 0.2, because $F_{S,c}$ decreases, and polymeric material possibly containing only HEMA is formed. This type of composition drift was also reported for the

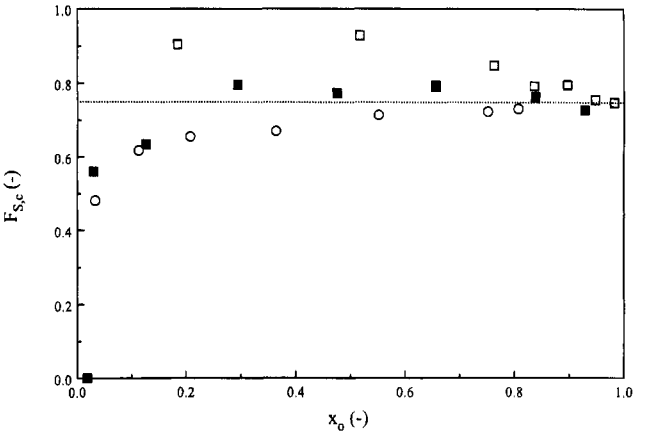


**Figure 5.** Cumulative fraction of S ($F_{S,c}$) (as determined with $^1$H NMR) in S–HEMA emulsion copolymers with $f_H$ = 0.25/$f_S$ = 0.75 and with varying M/W (g/g): 0.5 (○), 0.2 (■), and 0.05 (□).

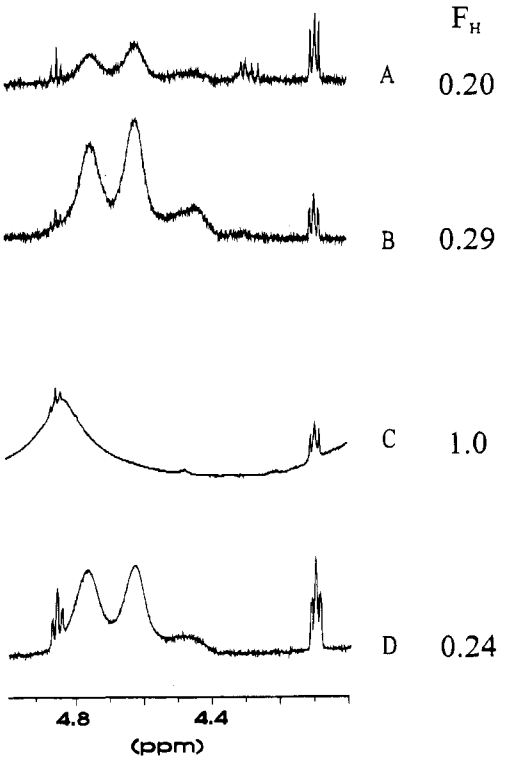


**Figure 6.** Expanded 400-MHz spectra hydroxyl proton signals of HEMA in $^1$H NMR spectra of two bulk copolymers of S and HEMA (A, $F_H$ = 0.20; B, $F_H$ = 0.29) and of two emulsion copolymers with an initial feed composition $f_H$ = 0.25 and M/W = 0.2 (C, $F_{H,c} = 1/x_0$ = 0.02; D, $F_{H,c} = 0.24/x_0$ = 0.86).

emulsion copolymerization of S and acrylamide by Ohtsuka *et al.*[20] It cannot be ruled out that indeed there are two homopolymerizations occurring at the same time. However, this is not in agreement with what was found in the CCDs of these copolymers. Looking at the NMR data in more detail may reveal more information.

*Comparison between Bulk Copolymers and Emulsion Copolymers.* In bulk copolymerization true copolymers are formed, as was convincingly shown above. The proton NMR spectra of these copolymers show that the signal of the hydroxyl proton in the HEMA units is split into three peaks X, Y, and Z at high fractions of S. This is again shown in Figure 6, where expanded 400-MHz proton NMR spectra of two low-conversion bulk copolymers with two different compositions ($F_H$ = 0.29 and 0.20) are given. Also shown are the corresponding parts

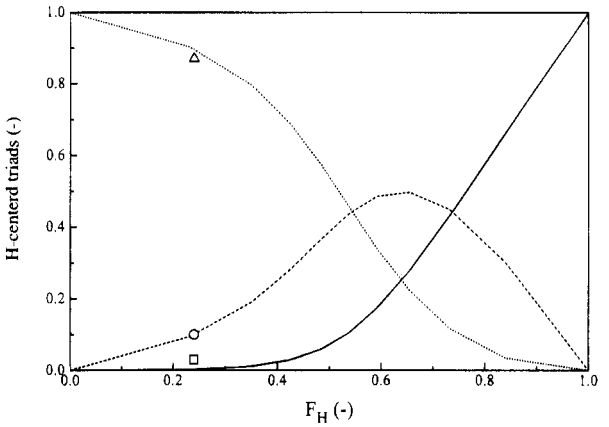


**Figure 7.** Variation with copolymer composition $F_H$ of the molar fractions of the HEMA-centered triads as calculated using $\sigma_{HS} = 0.33$ and $r_H = 0.48/r_S = 0.27$ (—, $F_{HHH}$; - - -, $F_{HHS}$; •••, $F_{SHS}$) and of the experimentally determined HEMA triads in the emulsion copolymer with M/W = 0.2, $x_0 = 0.86$, and $F_{H,c} = 0.24$ (□, $F_{HHH}$; ○, $F_{HHS}$, △, $F_{SHS}$).

of expanded 400-MHz NMR spectra of an emulsion copolymer of S and HEMA (M/W = 0.2, $f_H = 0.25$), sampled at two different overall conversions ($x_0$) and cumulative compositions ($F_{H,c}$). It can be seen that the three peaks X, Y, and Z into which the proton signal is split up in the bulk copolymers also show up in the high-conversion emulsion copolymer with a comparable overall composition Figure 6D). What's more, the relative intensities of each peak X, Y, and Z of the emulsion copolymer (Figure 6D) are comparable to the relative intensities in the bulk copolymers (Figure 6B). Figure 7 shows the variation of the molar fractions of HEMA-centered triads with the overall copolymer composition $F_H$ of a statistical copolymer. These triads have been calculated with eqs 3 and 4. The experimentally determined intensities of the peaks X, Y, and Z of the emulsion copolymer with M/W = 0.2, $x_0 = 0.86$, and $F_{H,c} = 0.24$ have been used to calculate the values of the HEMA-centered triad fractions in this emulsion by using eqs 2–4 and have also been given in Figure 7. It can be seen that there is good agreement between experimental and theoretical values, indicating that the emulsion copolymer with a cumulative composition of 0.24 has a microstructure almost equal to that of a bulk copolymer of the same composition. This can only mean that for the greater part of the reaction a true copolymer has been formed with a composition close to the cumulative composition at that conversion in Figure 4. This confirms what was seen in the CCDs, namely, that most of the polymeric material formed is a copolymer and that the position of the copolymer peak in the CCDs depends on the M/W: if two homopolymers would have been formed, the positions of the two peaks would be independent of M/W. The emulsion copolymer sample of low conversion (Figure 6C) with $F_{H,c} = 1$ and $x_0 = 0.02$ shows no splitting up of the hydroxyl signal. So at low conversion the polymer formed consists solely of HEMA. This polymer was probably formed in the aqueous phase. At high conversion, the fraction of S has increased rapidly. That this is not due to homopolymerization of S but to copolymerization with HEMA is proven by the fact that there appears a hydroxyl signal which is split into three peaks just as in the bulk copolymers and by the fact that the peak areas are in quantitative agreement with calculated values assuming the formation of a true copolymer.

In the present system it can be seen that although HEMA seems to be more reactive than S in bulk experiments, relatively S-rich copolymers are formed throughout the larger part of the reaction, because a relatively large part of HEMA is retained in the aqueous phase.[1] It should be noted that according to the NMR measurements this enrichment in S is not very high. At the beginning, where there are not enough polymer particles, and at the end when S has been depleted, HEMA-rich polymeric material is formed. The locus of polymerization probably shifts from the aqueous phase to the polymer phase at the beginning of the reaction, whereas the main locus of polymerization at the end of the reaction cannot be elucidated with these experiments. The fact that the HEMA-rich material is possibly also of low molecular weight, since in the CCD it could only be retraced at $F_S < 0$, may indicate that it is the aqueous phase, since in this phase the rate of termination is higher, but there is no evidence for this.

This copolymerization mechanism can account for the experimental data found by Kamei *et al.*[21] and by Okubo *et al.*[22]

## Conclusions

By analyzing the compositions of low-conversion bulk copolymers of styrene (S) and 2-hydroxyethyl methacrylate (HEMA) with proton NMR, the reactivity ratios of this comonomer pair at 50 °C could be determined by using the terminal model for propagation. The same model was successfully applied to interpret qualitatively and quantitatively the splitting up of the hydroxyl proton signal of the HEMA unit into three distinctive peaks. The three peaks could be easily assigned to a combination of the six possible compositional and configurational triads in a similar way as can be done with the methoxy proton signal in styrene–methyl acrylate copolymers. The coisotacticity parameter was found to be comparable with values found in other systems. Analysis of the chemical composition distribution of three emulsion copolymers of S and HEMA with gradient polymer elution chromatography and of the cumulative composition as a function of conversion with proton NMR suggests that the monomers copolymerize during the greater part of the reaction. Comparison of the hydroxyl proton signal in one of the emulsion copolymers with the hydroxyl proton signal in the corresponding bulk copolymers convincingly showed the presence of a significant amount of copolymer.

**Acknowledgment.** The authors express their gratitude to Jan van Hest, Bart Manders, and Alex van Herk.

## References and Notes

(1) Schoonbrood, H. A. S. Emulsion Co- and Terpolymerization, Monomer Partitioning Kinetics and Control of Microstructure and Mechanical Properties. Ph.D. Thesis, Eindhoven University of Technology, Eindhoven, The Netherlands, 1994.
(2) Schoonbrood, H. A. S.; Van Eijnatten, R. C. P. M.; van den Reijen, B.; German, A. L., submitted to *J. Polym. Sci.*
(3) Koenig, J. L. *Chemical Microstructure of Polymer Chains*; Wiley: New York, 1980.
(4) Harwood, H. J. Problems in Aromatic Copolymer Structure in Natural and Synthetic High Polymers. *NMR*; Diehl, P., Ed.; Springer-Verlag: Berlin, 1990; Vol. 4.
(5) Aerdts, A. M.; de Haan, J. W.; German, A. L.; van der Velden, G. P. M. *Macromolecules* **1991**, *24*, 1473 and references therein.
(6) Aerdts, A. M.; de Haan, J. W.; German, A. L. *Macromolecules* **1993**, *26*, 1965.

(7) Tackx, J. C. J. F.; van der Velden, G. P. M.; German, A. L. *J. Polym. Sci., Polym. Chem. Ed.* **1988**, *26*, 1439.
(8) van Doremaele, G. H. J.; German, A. L.; de Vries, N. K.; van der Velden, G. P. M. *Macromolecules* **1990**, *23*, 4206.
(9) Angad Gaur, H. *Recl. Trav. Chim. Pays-Bas* **1991**, *110*, 553.
(10) Llauro-Darricades, M. F.; Pichot, C.; Guillot, J.; Rios, G. L.; Cruz, M. A.; Guzman, C. *Polymer* **1986**, *27*, 889.
(11) Winter, H.; Barendswaard, W.; Neilen, M. G. M.; van der Velden, G. P. M. Proceedings of the 4th International Conference of Crosslinked Polymers, Luzern, May/June 1990, p 203.
(12) Gallardo, A.; San Román, J. *Polymer* **1994**, *35*, 2501.
(13) San Román, J.; Levenfeld, B. *Macromolecules* **1990**, *23*, 3036.
(14) San Román, J.; Levenfeld, B.; Madruga, E. L.; Vairon, J. P. *J. Polym. Sci., Polym. Chem. Ed.* **1991**, *29*, 1023.
(15) Mohan, D.; Radhakrishnan, G.; Rajadurai, S.; Joseph, K. T. *J. Polym. Sci., C: Polym. Lett.* **1990**, *28*, 307.
(16) Lebduška, J.; Šňupárek, J., Jr.; Kašpar, K.; Čermák, V. *J. Polym. Sci., Polym. Chem. Ed.* **1986**, *24*, 777.
(17) Galbraith, M. N.; Moad, G.; Solomon, D. H.; Spurling, T. H. *Macromolecules* **1987**, *20*, 675.
(18) Lebduška, J.; Šňupárek, J., Jr.; Čermák, V. *J. Polym. Sci., Polym. Lett. Ed.* **1984**, *22*, 261.
(19) Okubo, M.; Yamamoto, Y.; Uno, M.; Kamei, S.; Matsumoto, T. *Colloid Polym. Sci.* **1987**, *265*, 1061.
(20) Ohtsuka, Y.; Kawaguchi, H.; Sugi, Y. *J. Appl. Polym. Sci.* **1981**, *26*, 1637.
(21) Kamei, S.; Okubo, M.; Matsumoto, T. *J. Polym. Sci., Polym. Chem. Ed.* **1986**, *24*, 3109.
(22) Okubo, M.; Yamamoto, Y.; Kamei, S. *Colloid Polym. Sci.* **1989**, *267*, 861.
(23) Ketels, H.; Beulen, J.; van der Velden, G. P. M. *Macromolecules* **1988**, *21*, 2032.
(24) Van der Velden, G. P. M.; Beulen, J. *Macromolecules* **1982**, *15*, 1071.
(25) Toppet, S.; Slinkx, M.; Smets, G. *J. Polym. Sci., Polym. Chem. Ed.* **1975**, *13*, 1879.
(26) Plochocka, K.; Harwood, H. J. *Polym. Prepr. (Am. Chem. Soc., Div. Polym. Chem.)* **1978**, *19*, 240.
(27) Kim, S. Ph.D. Thesis, University of Akron, Akron, OH, 1990.
(28) Park, K. J.; Santee, E. R.; Harwood, H. J. *Polym. Prepr. (Am. Chem. Soc., Div. Polym. Chem.)* **1986**, *27*, 81.
(29) Sparidans, R. W.; Claessens, H. A.; van Doremaele, G. H. J.; German, A. L. *Chromatographia* **1990**, *31*, 493.
(30) Van Herk, A. M. *J. Chem. Educ.* **1995**, *72*, 138.
(31) Dube, M.; Amin Sanayei, R.; Penlidis, A.; O'Driscoll, K. F.; Reilly, P. M. *J. Polym. Sci., Polym. Chem. Ed.* **1991**, *29*, 703.
(32) Tidwell, P. W.; Mortimer, G. A. *J. Polym. Sci., Polym. Chem. Ed.* **1965**, *3*, 369.
(33) Van der Velden, G. P. M.; Beulen, J., private communications.
(34) Moritani, T.; Kuruma, I.; Shibatani, K.; Fiyiwara, J. *Macromolecules* **1972**, *5*, 577.
(35) Wu, T. K. *J. Polym. Sci., Polym. Phys. Ed.* **1976**, *14*, 343.
(36) Schoonbrood, H. A. S., unpublished results.
(37) Ito, K.; Iwase, S.; Umehara, K.; Yamashita, Y. *J. Macromol. Sci., Chem.* **1967**, *A1* (5), 891.

MA946314M